

pubs.acs.org/JACS Article

Rotational Spectra of Three Cyanobutadiene Isomers (C₅H₅N) of Relevance to Astrochemistry and Other Harsh Reaction Environments

Maria A. Zdanovskaia, P. Matisha Dorman, Vanessa L. Orr, Andrew N. Owen, Samuel M. Kougias, Brian J. Esselman, R. Claude Woods,* and Robert J. McMahon*



Cite This: J. Am. Chem. Soc. 2021, 143, 9551-9564



ACCESS

III Metrics & More

Article Recommendations

Supporting Information

ABSTRACT: Three cyanobutadiene isomers have been synthesized and their rotational spectra analyzed in the 130-375 GHz frequency range. These species, which are close analogues of known interstellar molecules and are isomers of the heterocyclic aromatic molecule pyridine (C_5H_5N) , offer the opportunity of revealing important insights concerning the chemistry in astronomical environments. The *s-trans* conformers of *E-1*-cyano-1,3-butadiene and *Z-1*-cyano-1,3-butadiene are observed, while both the *anti-clinal* and *syn-periplanar* conformers of 4-cyano-1,2-butadiene are evident in the rotational spectra. Over 1000 transitions for *s-trans-Z-1*-cyano-1,3-butadiene and for *syn-periplanar-4*-cyano-1,2-butadiene are fit to an octic, distorted-rotor Hamiltonian with low uncertainty (<50 kHz).



Although neither *s-trans-E-*1-cyano-1,3-butadiene nor *anti-clinal*-4-cyano-1,2-butadiene can be fully treated with a distorted-rotor Hamiltonian in this frequency range, we provide herein minimally perturbed, single-state least-squares fits of over 1000 transitions for each species, yielding sets of spectroscopic constants that are expected to enable accurate prediction of high-intensity transitions at frequencies up to 370 GHz for both isomers. The assigned transitions and spectroscopic constants for these cyanobutadienes have already enabled the identification of two isomers in harsh reaction environments and should be sufficient to enable their identification in astronomical environments by radio astronomy.

■ INTRODUCTION

Organic nitriles occupy a significant place in the field of astrochemistry. Their large molecular dipole moments confer rotational transitions with significant intensity, which facilitates identification of these species by radio astronomy. Recent detections of benzonitrile, the cyano-1,3-cyclopentadienes, and the cyanonaphthalenes represent a dramatic breakthrough in the field, ^{1–3} revealing a glimpse of simple aromatic compounds in astronomical environments. ⁴ We have been keenly interested in both structural and chemical relationships between open-chain organic nitriles and their cyclic counterparts for some time. ⁵ In the current investigation, we report millimeter-wave rotational spectra of three isomers of cyanobutadiene, which are also isomers of the heterocyclic aromatic molecule pyridine (C_5H_5N) .

Radio astronomy is the primary method of detecting molecules and ions in the interstellar medium (ISM) and circumstellar shells. ^{6,7} With their large dipole moments, nitriles (R–CN) are well represented in the list of ~220 species detected in space. The isomeric isocyanides/isonitriles (R–NC) are also polar, and many have been detected in the ISM despite being higher in energy by ~21 kcal/mol. The list of astronomically detected nitriles reveals variety in chain length ^{8–12} –from hydrogen cyanide (HCN)¹¹ to cyanodeca-

pentayne $(HC_{11}N)^{13}$ —as well as a variety in the level of saturation. As well as a variety in the level of saturation. For particular interest to the current work are vinyl cyanide (C_3H_3N) ; acrylonitrile), so cyanoallene $(C_4H_3N)^{17}$ and cyanodiacetylene $(HC_5N)^{8}$, which share structural elements with the cyanobutadiene isomers (C_5H_5N) of interest: E-1-cyano-1,3-butadiene, Z-1-cyano-1,3-butadiene, and 4-cyano-1,2-butadiene (Figure 1).

The structural similarity, and the fact that both smaller and larger carbon-chain nitriles are known in extraterrestrial environments, suggest that the cyanobutadiene isomers described in this work represent plausible targets for detection in the ISM. Recent studies examined potential routes to their formation. McCarthy *et al.* analyzed the products generated by electrical discharge of benzene and molecular nitrogen and identified both *E-* and *Z-1-cyano-1,3-butadiene* isomers in the product spectra (Figure 2a).²¹ Zwier and co-workers

Received: April 9, 2021 Published: June 22, 2021





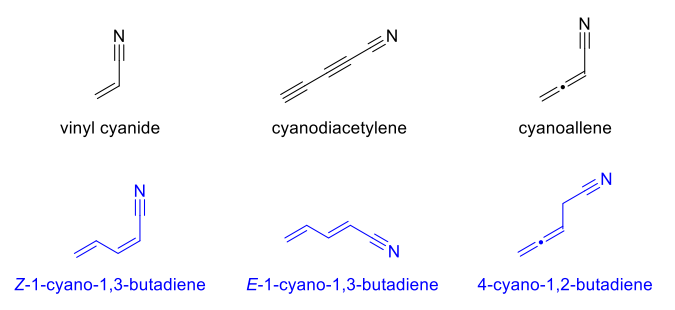


Figure 1. Molecules studied in this work (blue): *Z*-1-cyano-1,3-butadiene, *E*-1-cyano-1,3-butadiene, and 4-cyano-1,2-butadiene. Nitriles with similar structures that have been detected in the interstellar medium (black): vinyl cyanide, cyanodiacetylene, and cyanoallene.

Figure 2. (a) Discharge of benzene and nitrogen produces *E*-1-cyano-1,3-butadiene and *Z*-1-cyano-1,3-butadiene. (b) Pyrolysis of 1-cyano-2-butene produces *Z*-1-cyano-1,3-butadiene. (2)

investigated the gas-phase pyrolysis of trans-3-pentenenitrile, which results in dehydrogenation to afford Z-1-cyano-1,3butadiene, among many products (Figure 2b). Notably, pyridine was not detected, despite being lower in energy than the detected cyanobutadiene isomer. 22 The spectroscopic assignments in both of these experiments were made on the basis of data reported herein. Much earlier, Tsukamoto and Lichtin observed E- and Z-1-cyano-1,3-butadiene as products in a reaction between 1,3-butadiene and nitrogen activated via microwave discharge.²³ They noted the possibility that this reaction involves cyano radical as the primary intermediate. More recent theoretical and experimental studies indicate the reaction between cyano radical and 1.3-butadiene produces E-1-cyano-1,3-butadiene, despite the open-chain molecule being less thermodynamically favorable than pyridine. 24,25 Although the cyano radical has been known in the ISM for decades, 1,3-butadiene has not been detected. The predominant s-trans conformer does not possess a dipole moment, while the small dipole moment in the higher energy syn conformation makes it a difficult astronomical target.²⁷ Balucani et al. suggested that the reaction of cyano radical with an unsaturated hydrocarbon species is a highly plausible route to formation of the nitriles in the ISM, and that the detection of a particular unsaturated hydrocarbon can be used to predict the presence of the corresponding nitrile.²⁸ Given the small dipole moment of 1,3butadiene, however, it seems that the detection of the 1-cyano-1,3-butadiene isomers could better serve as potential tracers for 1,3-butadiene. A theoretical study by Jamal and Mebel²⁹ suggested that reaction of cyano radical with 1,2-butadiene would preferentially form 2-cyano-1,3-butadiene (C₅H₅N),³⁰ 1-cyano-3-propyne (C_4H_3N) , or cyanoallene (C_4H_3N) and not 4-cyano-1,2-butadiene. This does not preclude, however, generation of 4-cyano-1,2-butadiene by other reaction pathways.

The ISM is not the only location where detection of the cyanobutadiene isomers could be informative. Saturn's largest moon, Titan, possesses a nitrogen atmosphere with complex atmospheric chemistry and photochemistry. The atmospheric chemistry of Titan has been suggested to be relevant to prebiotic Earth.³¹ Small neutral nitriles, as well as their anions, have been detected in Titan's atmosphere and are implicated in the formation of tholins, 32-34 the organic polymers responsible for the reddish haze of various bodies in our solar system and suggested as potential prebiotic precursors in the presence of water. Pyrolysis of tholin analogues produces 1-cyano-1,3butadiene. 35,36 Data from the Cassini-Huygens probe also suggests the presence of benzene, 32,33 and data from the Atacama Large Millimeter Array (ALMA) recently revealed the presence of cyclopropenylidene.³⁷ It is likely that other aromatics like pyridine or its isomers could be detected in this environment.

With respect to astrochemistry, electrical discharge, or other harsh reaction environments, the cyanobutadiene isomers (Figure 1) are important in that they may be considered proxies for pyridine. Pyridine is an aromatic molecule of substantial astrochemical interest that has thus far eluded detection in the ISM.³⁸ The cyanobutadiene isomers are more polar ($\mu = 3.7-4.7$ D), and therefore more readily detectable, than pyridine ($\mu = 2.2$ D). Mechanistically, it is not known whether the cyanobutadiene isomers might represent precursors to pyridine or decomposition products of pyridine, but the detection of any isomer of pyridine (C5H5N) would represent a significant observation in astrochemistry.^{39–41} Pyridine is nearly 23.2 kcal/mol lower in energy than E-1cyano-1,3-butadiene, which itself is 0.3 and 16.3 kcal/mol lower in energy than Z-1-cyano-1,3-butadiene and 4-cyano-1,2butadiene (B3LYP/6-311+G(2d,p)), respectively. Pyridine is a building block of nicotinic acid (vitamin B3) and nicotinamide, which are precursors to a key coenzyme used in metabolism, nicotinamide adenine dinucleotide (NAD).⁴² A possible route to interstellar formation of nicotinic acid from pyridine has been suggested, 43 and nicotinic acid of interstellar origin has been detected on the Murchison meteorite. 44,45 Identification of extraterrestrial pyridine could assist our understanding of prebiotic chemistry occurring in extreme environments as well as our understanding of formation of nitrogen-containing polycyclic aromatic hydrocarbons (NPAHs), in which pyridine has been suggested as a precursor.⁴⁶

Herein, we present a detailed analysis of the rotational spectra of the ground vibrational states of E-1-cyano-1,3butadiene, Z-1-cyano-1,3-butadiene, and 4-cyano-1,2-butadiene in the 130-375 GHz frequency range. These experimental studies are predicated on the availability of pure samples of the neat materials, which is not an inconsequential matter.⁴⁷ These laboratory measurements provide the foundation for spectroscopic studies of astronomical and other harsh reaction environments. Interstellar detection involves astronomical measurement of either (i) transitions that have been directly measured in the laboratory or (ii) transitions that have been predicted, with high precision, on the basis of experimentally determined spectroscopic constants. The transition frequencies and spectroscopic constants determined in the current investigation provide a sufficient basis for radio astronomy searches for these species from radio- to millimeter-wave frequencies.

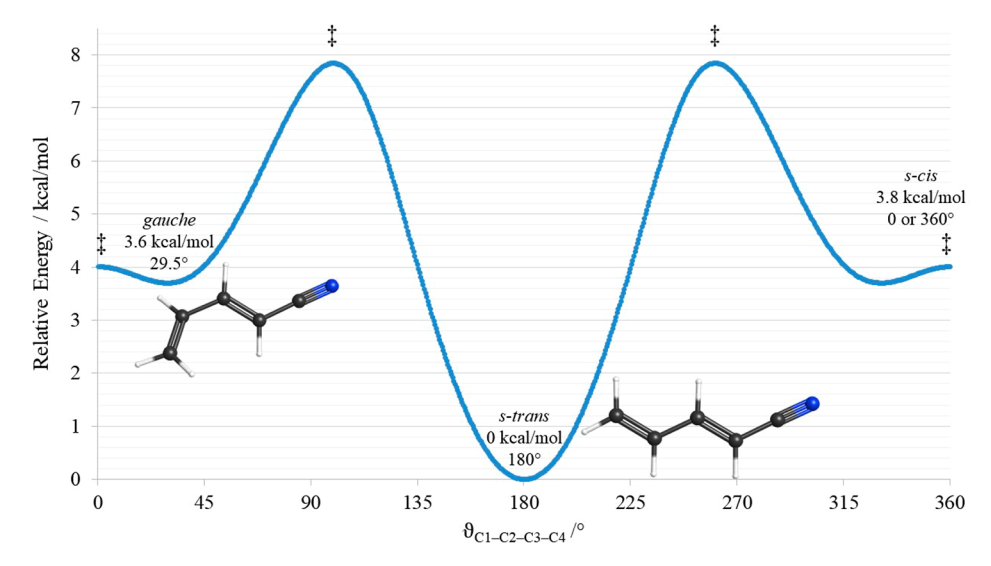


Figure 3. Computed conformational potential energy surface of E-1-cyano-1,3-butadiene (B3LYP/6-311+G(2d,p)).

■ MATERIALS AND METHODS

Experimental Methods. The cyanobutadiene isomers were synthesized in our lab as described previously.⁴⁷ collected on a broadband spectrometer using 3-13 mTorr sample pressures in a flow system at 0 to -50 °C. Liquid samples of all three cyanobutadiene isomers were kept in ice-water baths to minimize sample degradation. The (high) purity of each sample was established on the basis of ¹H NMR and mass spectra. ⁴⁷ No impurities were evident in the rotational spectra. Transitions observed in the rotational spectra are associated with the designated molecule (ground state, vibrationally excited states, isotopologues detectable in natural abundance, and minor conformational isomers). The 130-230 and 235–375 GHz spectra were collected by using an instrument described previously 48,49 and two separate Virginia Diodes amplification and multiplication chains and zero-bias detectors. The spectra were combined into a single broadband spectrum by using Assignment and Analysis of Broadband Spectra (AABS) software. 50 Pickett's SPFIT/SPCAT programs $^{\rm 52}$ and Kisiel's ASFIT/ASROT $^{\rm 50,51}$ were used to conduct least-squares fitting and spectral prediction. PIFORM, PLANM, and AC programs⁵³ were used for data analysis, file formatting, and generating various plots and graphics.

In our least-squares fits, we assume a uniform frequency measurement uncertainty of 50 kHz for our data. Transitions from McCarthy *et al.*²¹ use an uncertainty of 2 kHz, and those from Mishra *et al.*²² use 60 kHz.

Computational Methods. Computations were performed at the B3LYP/6-311+G(2d,p) level of theory by using Gaussian 16.⁵⁴ Optimized geometries were obtained by using "verytight" convergence criteria and an "ultrafine" integration grid for each of the energy-minimized conformers of *E*-1-cyano-1,3-butadiene, *Z*-1-cyano-1,3-butadiene, and 4-cyano-1,2-butadiene. Anharmonic vibrational frequency calculations provided predictions of vibration—rotation interaction constants and quartic and sextic centrifugal distortion constants, as well as fundamental frequencies of the vibrationally excited states. Coordinate scans for rotation about the C2—C3 bond for the 1-cyano-1,3-butadiene isomers and the C3—C4 bond for 4-cyano-1,2-butadiene were computed at the same level of theory. Computational output files are provided in the Supporting Information.

RESULTS AND DISCUSSION

Analysis of Rotational Spectra. *E-1-Cyano-1,3-butadiene*. *E-1-Cyano-1,3-butadiene* exhibits two low-energy conformations: *s-trans* and *gauche*, depicted on the conformational potential energy surface in Figure 3. The latter conformer has a predicted C1–C2–C3–C4 dihedral angle



Figure 4. *s-trans-E-1-Cyano-1,3-*butadiene structure with principal inertial axes ($\mu_a = 4.6$ D, $\mu_b = 1.0$ D).

of 29.5°, which is reasonably close to the corresponding dihedral angle experimentally determined for 1,3-butadiene $(33.8 \pm 1.3^{\circ})^{27}$ s-trans-E-1-Cyano-1,3-butadiene is favored by \sim 3.6 kcal/mol or 1259 cm⁻¹ (B3LYP/6-311+G(2d,p)) and is observed in the rotational spectrum. The predicted energy difference in the conformers indicates that the gauche conformer is ~0.3% as abundant as the s-trans at room temperature. Although the transition intensity of the gauche conformer would be statistically doubled by the presence of enantiomers, the small energy barrier between the two conformations (0.2 kcal/mol or 70 cm⁻¹; B3LYP) would possibly result in tunneling splitting, diminishing the transition intensity. These factors, taken together with the similar dipole moments of the gauche ($\mu_a = 4.6 \text{ D}$, $\mu_b = 0.2 \text{ D}$, $\mu_c = 0.2 \text{ D}$) and the s-trans ($\mu_a = 4.6$ D, $\mu_b = 1.0$ D) conformer and the very dense spectrum of s-trans-E-1-cyano-1,3-butadiene, make it unsurprising that gauche-E-1-cyano-1,3-butadiene was not observed in the rotational spectrum.

The *s-trans* conformer of *E*-1-cyano-1,3-butadiene, depicted in Figure 4, is a planar (C_s) , prolate $(\kappa = -0.99)$, asymmetric top with its dipole moment predominantly along the *a* principal axis. The lowest-energy vibrationally excited state is predicted to be 137 cm⁻¹ higher in energy than the ground state and is close in energy to the second-lowest energy vibrationally excited state (141 cm^{-1}) .

The rotational spectrum of *s-trans-E-1-cyano-1,3-butadiene* in the 130–370 GHz region is dominated by ${}^{a}R_{0,1}$ transitions that appear in clusters of transitions sharing a single J value. A small portion of the spectrum is shown in Figure 5. Such a band structure is typical for a highly prolate, asymmetric top, and bands throughout our spectral region follow the same pattern. Although the $K_a = 0$ and 1 transitions of the J'' + 1 = 119 series appear near the middle of this region, and several

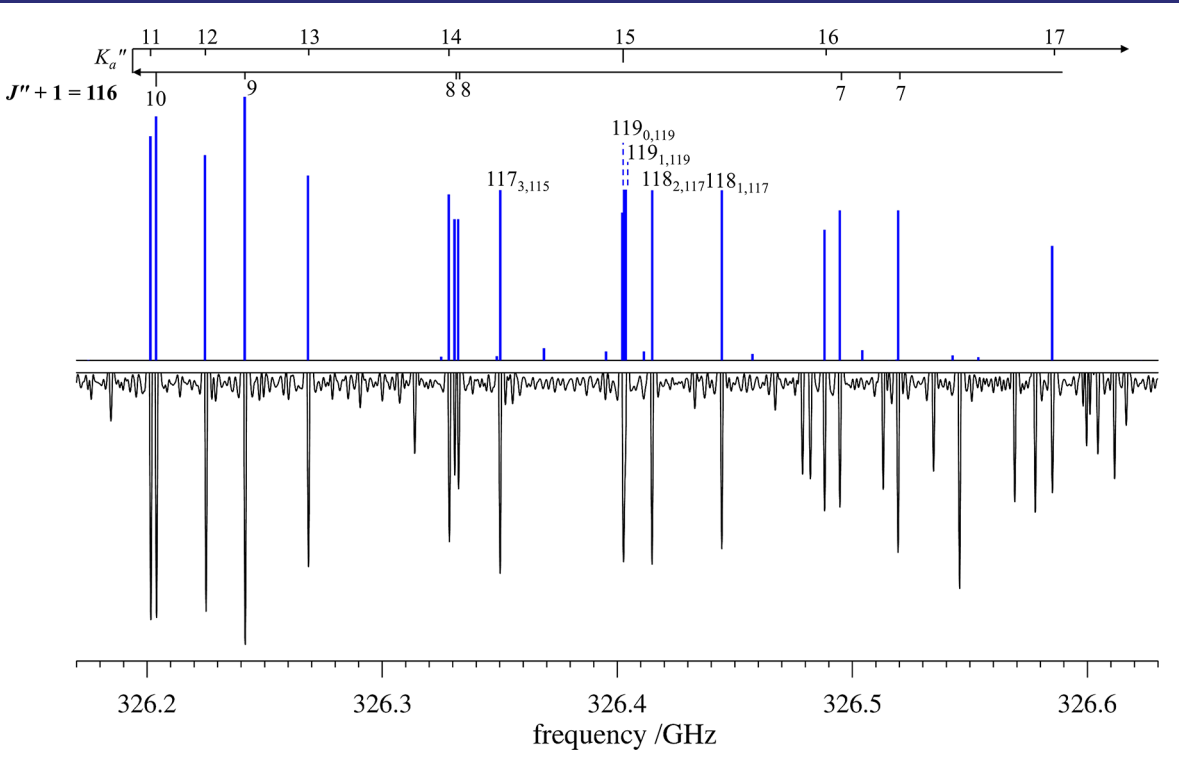


Figure 5. Rotational spectrum of *s-trans-E-*1-cyano-1,3-butadiene from 326.17 to 326.63 GHz (bottom) and stick spectrum of the ground vibrational state transitions (top). The upper state J (i.e., J'' + 1) value for most transitions in this region is 116; K_a values for this series are denoted at the top. The upper state quantum numbers of the five ${}^aR_{0,1}$ transitions not belonging to the J'' + 1 = 116 series are marked immediately above their stick spectrum positions. Many transitions belonging to other vibrational satellites are also visible in the experimental spectrum.

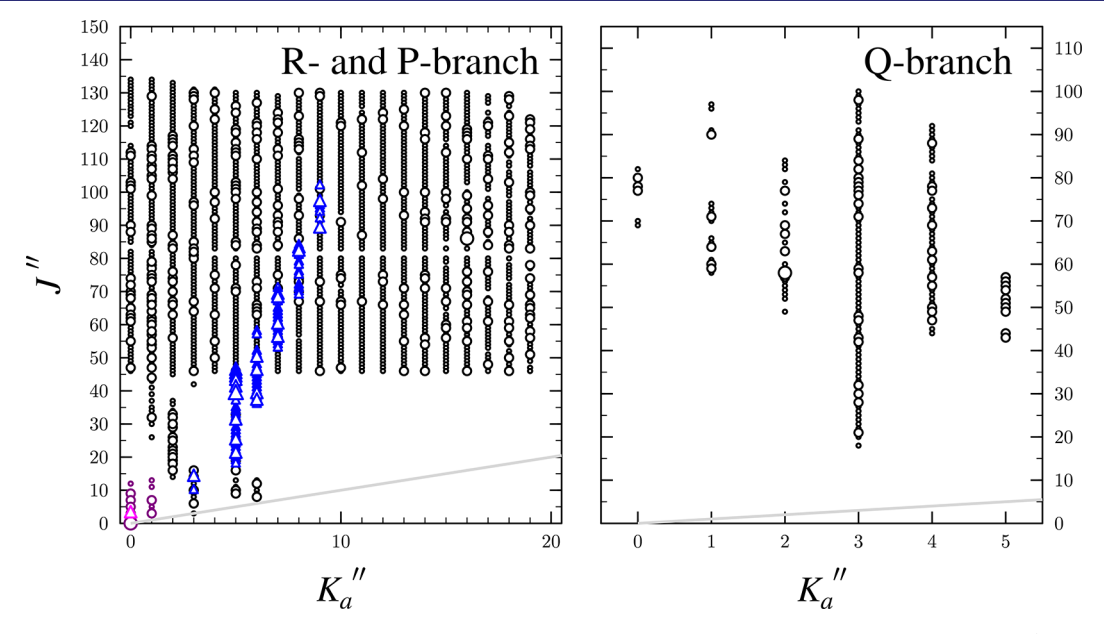


Figure 6. Data distribution plot for the minimally perturbed least-squares fit of spectroscopic data from the current work (black and blue) and measurements from McCarthy *et al.*²¹ (purple and magenta) for the vibrational ground state of *s-trans-E-1*-cyano-1,3-butadiene. Circles indicate Q- and R-branch transitions. Triangles indicate P-branch transitions. The size of the plotted symbol is proportional to the value of $|(f_{obs} - f_{calc})/\delta f|$, where δf is the frequency measurement uncertainty; all values shown are smaller than 3.

transitions with increasing values of K_a and decreasing J are present, the majority of the transitions in the cluster have a value of J'' + 1 = 116. The $K_a = 0$ transition of the J'' + 1 = 116 series appears ~ 8 GHz lower in frequency than the depicted spectral region and is not degenerate with any other transition. With increasing values of K_a , transitions appear at higher frequencies up to ~ 329.5 GHz, which marks a turnaround at

 $K_a = 4$. Transitions sharing the same values of J and K_a , but with values of K_c differing by one, become degenerate at $K_a = 9$ for the given series. Another turnaround, which appears in the depicted spectral region, occurs at $K_a = 11$. Other bands in our frequency region follow a similar pattern. Though they are less intense than the a-type transitions, b-type R-branch transitions are also observed. Q-branch transitions, which occur in clusters

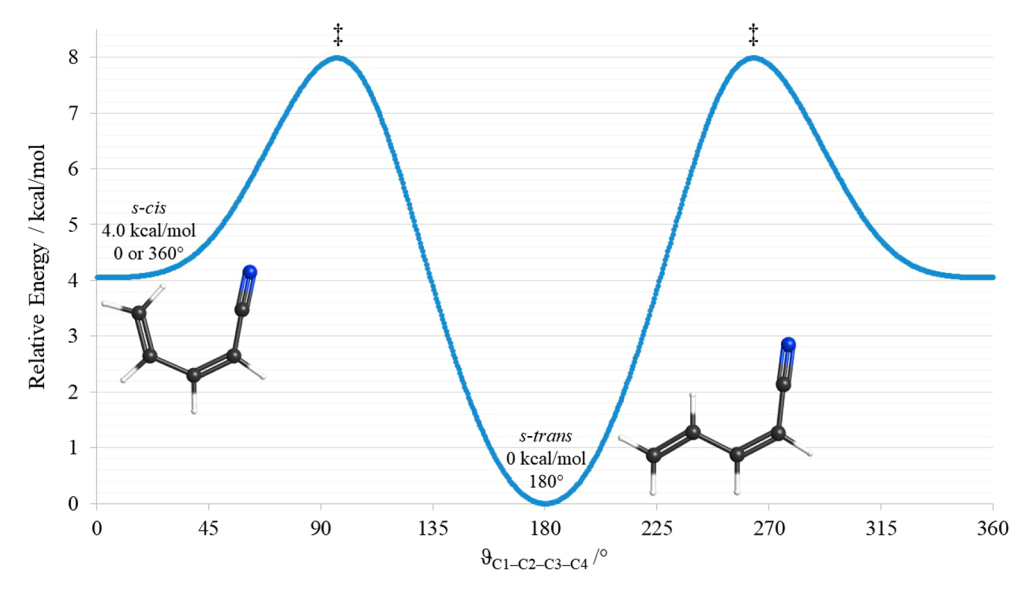


Figure 7. Computed conformational potential energy surface of Z-1-cyano-1,3-butadiene (B3LYP/6-311+G(2d,p)).

Table 1. Experimental and Computational Spectroscopic Constants for the Ground Vibrational State of *s-trans-E-1*-Cyano-1,3-butadiene (C₅H₅N) (S-Reduced Hamiltonian, I^r Representation)

_					
	B3LYP ^a	experimental b,c			
A_0 (MHz)	27003	26243.02934 (59)			
B_0 (MHz)	1437	1443.620880 (19)			
C_0 (MHz)	1364	1368.119206 (18)			
D_{J} (kHz)	0.11	0.1208886 (39)			
D_{JK} (kHz)	-14.9	-15.71829 (18)			
D_K (kHz)	1107.1	1106.785 (15)			
d_1 (kHz)	-0.016	-0.01794561 (99)			
d_2 (kHz)	-0.00029	-0.00041621 (28)			
H_j (Hz)	0.000068	0.00008551 (35)			
H_{JK} (Hz)	-0.015	-0.017117 (23)			
H_{KJ} (Hz)	-0.199	-0.0618 (14)			
H_K (Hz)	73.1	69.63 (11)			
h_1 (Hz)	0.000021	0.000024998 (45)			
h_2 (Hz)	0.00000068	0.000001168 (28)			
h_3 (Hz)	0.00000038	0.000000544 (15)			
L_J ($\mu { m Hz}$)		-0.000129 (10)			
$L_{JJK}~(\mu { m Hz})$		0.02058 (75)			
$L_{JK}~(\mu { m Hz})$		-2.594(47)			
$L_{K\!K\!J}~(\mu{ m Hz})$		-238.5 (39)			
χ_{aa} (MHz)	-3.7^{d}	-3.329 (19)			
$\chi_{bb}~({ m MHz})$	1.5 ^d	1.280 (25)			
$\Delta_i (u \mathring{A}^2)^{e,f}$		0.061888 (7)			
$N_{ m lines}{}^{m{g}}$		2644			
$\sigma_{ m fit}~({ m MHz})$		0.036			

"Evaluated with the 6-311+G(2d,p) basis set. ^bGlobal fit to the present minimally perturbed millimeter wave measurements (2600 independent transitions) and the available literature data (44 independent transitions from McCarthy et al. ²¹). ^cConstants not shown explicitly were held fixed at a value of zero. ^dConstants converted from the field gradient axis system to the inertial moment axis system. ^eInertial defect, $\Delta_i = I_c - I_a - I_b$, ^fCalculated by using PLANM from the B_0 constants. ^gNumber of fitted transition frequencies.

sharing the same K_a value, and widely spaced P-branch transitions are also observed in the spectrum.



Figure 8. *s-trans-Z-*1-Cyano-1,3-butadiene structure with principal inertial axes ($\mu_a = 3.6$ D, $\mu_b = 2.3$ D).

Although the rotational spectrum of s-trans-E-1-cyano-1,3butadiene appears well-behaved at low K_a , those series near K_a = 20 appear curved in Loomis-Wood plots and increasingly deviate from predicted frequencies at higher values of J. While many such series of R-, Q-, and P-branch transitions can be assigned, it is clear that their energy levels are perturbed and thus not amenable to a single-state least-squares fit. Many of these assignable, but highly perturbed transitions are excluded from the data set provided here (vide infra). Assigned transitions in the data set provided here include R-branch transitions ranging in J'' from 3 to 134 and in K_a'' from 0 to 19, Q-branch transitions with values of J'' from 18 to 100 and K_a'' from 0 to 5, and P-branch transitions with values of J'' from 3 to 102 and K_a " from 3 to 9. Although this is not a complete transition list and transitions could certainly be added if the spectrum were properly analyzed with a Hamiltonian addressing the coupling, the most intense transitions—those that would be most useful to anyone seeking this molecule in a reaction or extraterrestrial spectrum—are assigned and included in the data provided here. A coupled-state leastsquares fit is in progress. In an attempt to acquire minimally perturbed, reasonably realistic constants, we excluded all transitions with $K_a'' \ge 20$, numerous transitions with $K_a'' > 1$ 15 at high J, and transitions with error greater than 0.1 MHz. A data distribution plot demonstrating the breadth of data included in this minimally perturbed least-squares fit is presented in Figure 6.

In this work, we provide a set of spectroscopic constants that includes a full set of quartic and sextic centrifugal distortion constants, along with a partial set of octic constants, for *s-trans*-

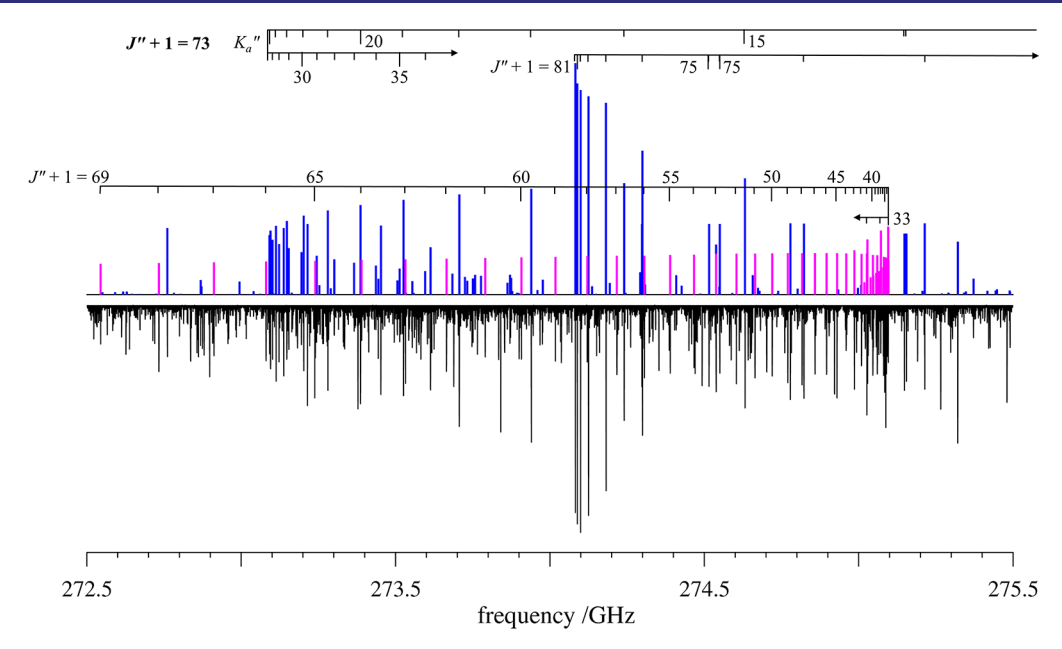


Figure 9. Rotational spectrum of *s-trans-Z*-1-cyano-1,3-butadiene from 272.50 to 275.50 GHz (bottom) and stick spectrum of the ground vibrational state transitions (top). Blue transitions denote R-branch transitions, while magenta transitions belong to the Q-branch. The upper state J (*i.e.*, J'' + 1) values are marked immediately above their stick spectrum positions. Many transitions belonging to other vibrational satellites are also visible in the experimental spectrum.

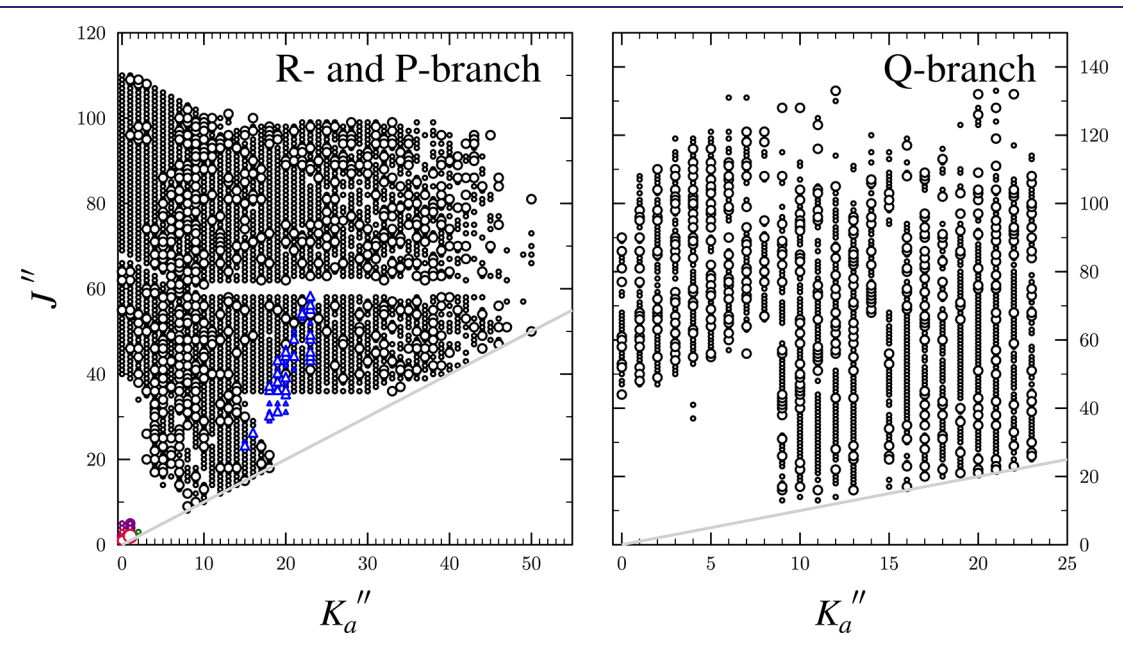


Figure 10. Data distribution plot for the least-squares fit of spectroscopic data from the current work (black and blue), measurements from McCarthy et al. 21 (purple and red, due to the high relative error), and measurements from Mishra et al. 22 (green) for the vibrational ground state of s-trans-Z-1-cyano-1,3-butadiene. Circles indicate Q- and R-branch transitions. Triangles indicate P-branch transitions. The size of the plotted symbol is proportional to the value of $|(f_{\text{obs}} - f_{\text{calc}})/\delta f|$, where δf is the frequency measurement uncertainty. For several precisely measured low-J'' and low- K_a transitions, the relative error is greater than 3 (red).

E-1-cyano-1,3-butadiene, fit with low error ($\sigma_{\rm fit}$ = 0.036 MHz). Although this least-squares fit does not address the coupling observed in our frequency range, we expect that the constants are minimally affected by perturbation and physically meaningful. A comparison of the predicted rotational and distortion constants with those from the minimally perturbed least-squares fit is provided in Table 1, and the resultant fit file is provided in the Supporting Information. The predicted rotational constants are within 3% of the minimally perturbed fit constants, and the quartic distortion constants, with the

exception of d_2 , are within 11%. Meanwhile, d_2 deviates from the experimental value by 31%, but its value is also quite small—100× smaller than the next smallest quartic distortion constant. As a result, it is correspondingly difficult to predict its value with a small relative error. This situation is, in fact, very similar to that observed for syn-2-cyano-1,3-butadiene. The sextic distortion constants are also well predicted and within 42% of the effective fit values, except H_{KJ} , which is about 3 times larger than its experimental value. The predicted constants are in good agreement with those determined

Table 2. Experimental and Computational Spectroscopic Constants for the Ground Vibrational State of s-trans-Z-1-Cyano-1,3-butadiene (C_5H_5N) (S-Reduced Hamiltonian, I^r Representation)

	B3LYP ^a	experimental ^b		
A_0 (MHz)	10155	9759.44594 (25)		
B_0 (MHz)	1983	2039.686938 (29)		
C_0 (MHz)	1658	1686.177389 (28)		
D_{J} (kHz)	0.75	0.8175616 (81)		
D_{IK} (kHz)	-12.3	-11.904999 (55)		
D_K (kHz)	78.0	68.8804 (15)		
d_1 (kHz)	-0.22	-0.2426311 (30)		
d_2 (kHz)	-0.0090	-0.01140453 (74)		
H_I (Hz)	0.000799	0.0007551 (11)		
H_{lK} (Hz)	0.0027	0.0076984 (74)		
H_{KI} (Hz)	-0.385	-0.390414 (51)		
H_K (Hz)	2.45	2.1490 (35)		
h_1 (Hz)	0.000395	0.00039284 (36)		
h_2 (Hz)	0.000058	0.00007271 (15)		
h_3 (Hz)	0.0000113	0.000014285 (32)		
L_{I} (μHz)		0.000709 (46)		
L_{IJK} (μHz)		-0.08232 (29)		
L_{JK} (μHz)		-0.0230 (43)		
L_{KKJ} (μHz)		13.293 (17)		
$L_K (\mu Hz)$		-97.1 (2.8)		
$l_1 \; (\mu \text{Hz})$		0.000237 (13)		
$l_2 \; (\mu \text{Hz})$		-0.0002057 (77)		
$l_3 (\mu Hz)$		-0.0000505 (28)		
$l_4~(\mu { m Hz})$		-0.00001450 (55)		
χ_{aa} (MHz)	-0.8^{c}	-0.3586 (55)		
χ_{bb} (MHz)	-1.4^{c}	-1.651 (15)		
$\Delta_i (u \mathring{A}^2)^{d,e}$		0.162360 (6)		
$N_{ m lines}^{\ \ f}$	5531			
$\sigma_{ m fit} \; ({ m MHz})$	0.038			
		h		

"Evaluated with the 6-311+G(2d,p) basis set. ^bGlobal fit to the present millimeter wave measurements (5495 independent transitions) and the available literature data (34 independent transitions from McCarthy et al.²¹ and 2 independent transitions from Mishra et al.²²). ^cConstants converted from the field gradient axis system to the inertial moment axis system. ^dInertial defect, $\Delta_i = I_c - I_a - I_b$. ^eCalculated by using PLANM from the B_0 constants. ^fNumber of fitted transition frequencies.

experimentally. There are no computational or previously determined octic centrifugal distortion constants to serve as an external reference, but we believe the octic constants determined here do not serve as strictly empirical corrections, nor do they absorb unaddressed perturbations because of the previously described efforts to avoid effects of perturbation.

The quadrupole coupling constants presented in Table 1 are obtained by including the low-frequency, hyperfine-resolved data from McCarthy $et\ al.^{21}$ in our least-squares fit. No new hyperfine-resolved transitions were added in the current work, as transitions affected by the nitrogen quadrupole are not resolvable in our frequency range. The values reported here vary somewhat from those based solely on the lower-frequency data due to our more accurate determination of the distortion constants, which decreases the convolution of quadrupole coupling and distortion in the least-squares fit. The small, but nonzero, value of the inertial defect (Δ_i) is within the range expected for a planar molecule. Although the inertial defect derived from the *equilibrium* rotational constants of a planar molecule should be precisely zero, the *measured* rotational

constants reported in Table 1 are affected by vibration—rotation interaction and the electron-mass distribution in the molecule.

Z-1-Cyano-1,3-butadiene. Z-1-Cyano-1,3-butadiene is predicted to exhibit two low-energy conformations: s-trans and scis, depicted on the conformational potential energy surface in Figure 7. It is well established that B3LYP calculations tend to overestimate stabilization due to π conjugation, so it is conceivable that the s-cis conformation may actually be a transition state separating enantiomeric gauche conformers, in a situation analogous to that predicted for the E-isomer and observed for 1,3-butadiene.^{27*}The s-cis conformer is 4.0 kcal/ mol (1399 cm⁻¹) higher in energy than the s-trans conformer, which would make the former ~0.1% the abundance of the latter at room temperature. Considering also the comparable dipole moment of the s-cis conformer ($\mu_a = 3.7$, $\mu_b = 2.4$) relative to the s-trans ($\mu_a = 3.6$ D, $\mu_b = 2.3$ D) and the possibility of tunneling splitting if the s-cis conformer is indeed a transition state, it is not surprising that the s-trans conformer is the only species observed in the rotational spectrum.

s-trans-Z-1-Cyano-1,3-butadiene, depicted in Figure 8, is a prolate ($\kappa = -0.91$), asymmetric top with C_s symmetry. The lowest-energy vibrationally excited state is predicted to be 129 cm⁻¹ higher in energy than the ground state and is close in energy to the second-lowest-energy vibrationally excited state (135 cm⁻¹).

In our frequency region, the most intense rotational transitions in the ground vibrational state are part of the oblate-structure R-branch bandhead, where a- and b-type transitions (${}^aR_{0,1}$, ${}^bR_{1,1}$, and ${}^bR_{1,-1}$) with the same value of K_c are quadruply degenerate. An example of such a bandhead is provided in Figure 9. Near the bandhead, transitions with increasing values of K_a occur at higher frequency and become nondegenerate. Because of the substantial a- and b-dipole moments, both types of transitions are observed, even when they are nondegenerate. Eventually, ${}^aR_{0,1}$ transitions with the same value of K_a become degenerate and coalesce into rolate series with the same values of J, as do ${}^bR_{1,1}$ with ${}^bR_{1,-1}$ transitions. Such a prolate aR -branch series for J'' + 1 = 73 is also apparent in the spectrum in Figure 9. Q-branch and P-branch transitions are visible across our spectral region as well.

Notably different between the s-trans conformers of Z- and E-1-cyano-1,3-butadiene is the apparent lack of coupling in the ground state of the Z isomer. The ground-state rotational spectrum of s-trans-Z-1-cyano-1,3-butadiene was successfully fit to a full octic, distorted-rotor Hamiltonian with low error ($\sigma_{\rm fit}$ = 0.039 MHz). A total of 5495 new independent transitions were assigned in the 130-375 GHz frequency region. The full data set, including recently reported transitions from McCarthy et al.21 and Mishra et al.,22 encompasses Rbranch transitions with K_a values ranging from 0 to 50 and J''values from 1 to 110 with no evidence of perturbation. Numerous a- and b-type Q-branch series, with J" values from 13 to 133 and K_a values from 0 to 23, were fit, along with a few weak P-branch transitions with J" values ranging from 23 to 58 and K_a values from 15 to 23. The data distribution plot for transitions of s-trans-Z-1-cyano-1,3-butadiene fit in this work is provided in Figure 10.

The current work provides spectroscopic constants, including full sets of sextic and octic centrifugal distortion constants, for *s-trans-Z-1-cyano-1,3-butadiene* (Table 2; S reduction, I^r representation). The resultant fit files and a comparison of A reduction constants to those recently

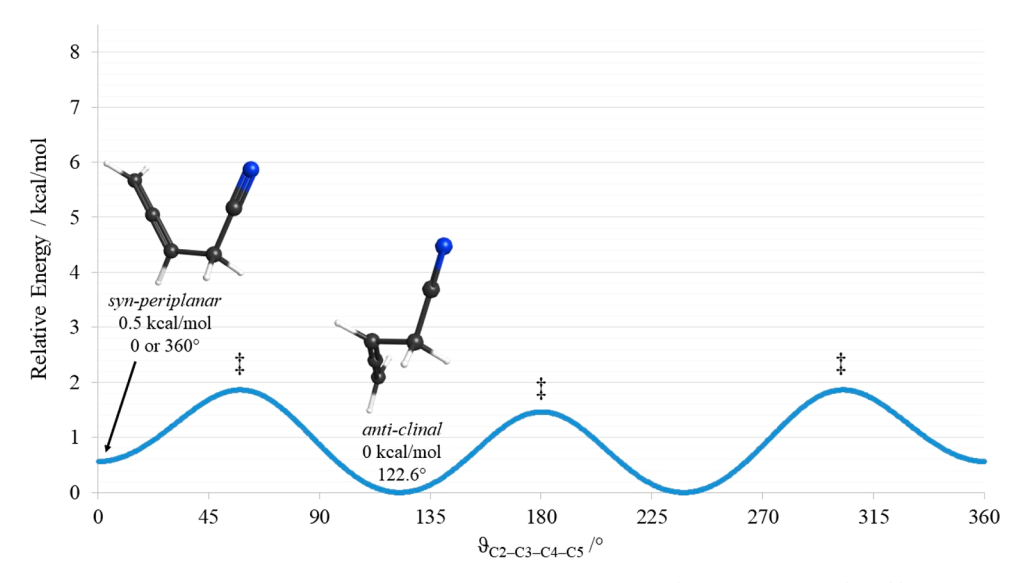


Figure 11. Computed conformational potential energy surface of 4-cyano-1,2-butadiene (B3LYP/6-311+G(2d,p)).

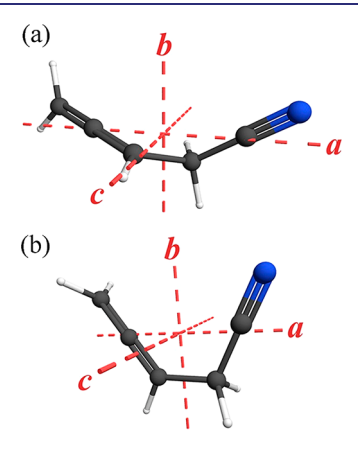


Figure 12. 4-Cyano-1,2-butadiene structures with principal inertial axes: (a) *anti-clinal* (μ_a = 3.6 D, μ_b = 1.9 D, μ_c = 0.6 D) and (b) *syn-periplanar* (μ_a = 2.0 D, μ_b = 3.1 D).

published by McCarthy et al.²¹ are provided in the Supporting Information. The experimentally determined distortion constants are expected to be physically meaningful and accurate in view of the very large number of transitions and lack of observed perturbation. Overall, the spectroscopic constants predicted by the B3LYP anharmonic calculation are reasonably good estimates of the experimental constants. The predicted rotational constants are within 4.2% of the experimentally determined values. The quartic centrifugal distortion constants are predicted within 21.4%, which is the error on the smallest of the constants, and the sextic constants are predicted to within 65% of their experimentally determined values. Again, no computational software currently predicts the octic centrifugal distortion constants, and no published data are available that would provide an external comparison. Data for the quadrupole coupling constants are based on the hyperfineresolved transitions measured by McCarthy et al. 211 These values are very close to those based solely on the lowerfrequency data (in fact, these values are within the uncertainty of the previous values), and the slight difference can be attributed to the improved determination of the distortion constants in this work. The value of the inertial defect (Δ_i) for the Z isomer is reasonable for a planar molecule. The

difference between the inertial defects for the Z and E isomers (\sim 0.1 uÅ²) is likely due to differences in vibration—rotation interactions and is not indicative of structural differences, *i.e.*, degree of deviation from planarity.

4-Cyano-1,2-butadiene. 4-Cyano-1,2-butadiene exhibits two low-energy conformations: syn-periplanar (syn-) and anticlinal (anti-), depicted on the conformational potential energy surface in Figure 11. The computed energy difference between the two conformers is quite small; the syn-periplanar conformer is only ~0.5 kcal/mol (175 cm⁻¹) higher in energy than the anti-clinal conformer—a value that is within the uncertainty of the level of theory employed. As a consequence of the small energy difference and the low barriers to internal rotation, both conformers are expected to be observable in the room temperature rotational spectrum. The transition intensities of anti-4-cyano-1,2-butadiene benefit from statistical doubling due to the presence of enantiomeric forms.

anti-4-Cyano-1,2-butadiene (Figure 12a) is a prolate ($\kappa = -0.99$), asymmetric top with C_1 symmetry and substantial dipole moment components along both the a and b principal axes ($\mu_a = 3.6$ D, $\mu_b = 1.9$ D, $\mu_c = 0.6$ D). The lowest-energy vibrationally excited state (the torsion) is predicted to be only 53 cm⁻¹ higher in energy than the ground vibrational state. syn-4-Cyano-1,2-butadiene (Figure 12b) is a less prolate ($\kappa = -0.60$), asymmetric top with C_s symmetry and substantial dipole moment components along both the a and b principal axes ($\mu_a = 2.0$ D, $\mu_b = 3.1$ D). The lowest-energy vibrationally excited state (also the torsion) is predicted to be 86 cm⁻¹ higher in energy than the ground vibrational state.

The 130–375 GHz rotational spectrum of 4-cyano-1,2-butadiene reveals the presence of both anti and syn conformers. The most intense rotational transitions in the spectrum are the aR transitions of the anti conformer (Figure 13). The $K_a=0$ and 1 transitions are nondegenerate in our frequency region, although the two a-type transitions with the same value of K_c become near-degenerate at the top of the observed frequency region. Transitions of individual bands at low K_a are spread sufficiently far that it is difficult to discern the pattern, but transitions sharing the same value of I and the same value of I and structure becomes distinguishable. Lower-intensity, I-type I-branch transitions and I-branch transitions are also observable

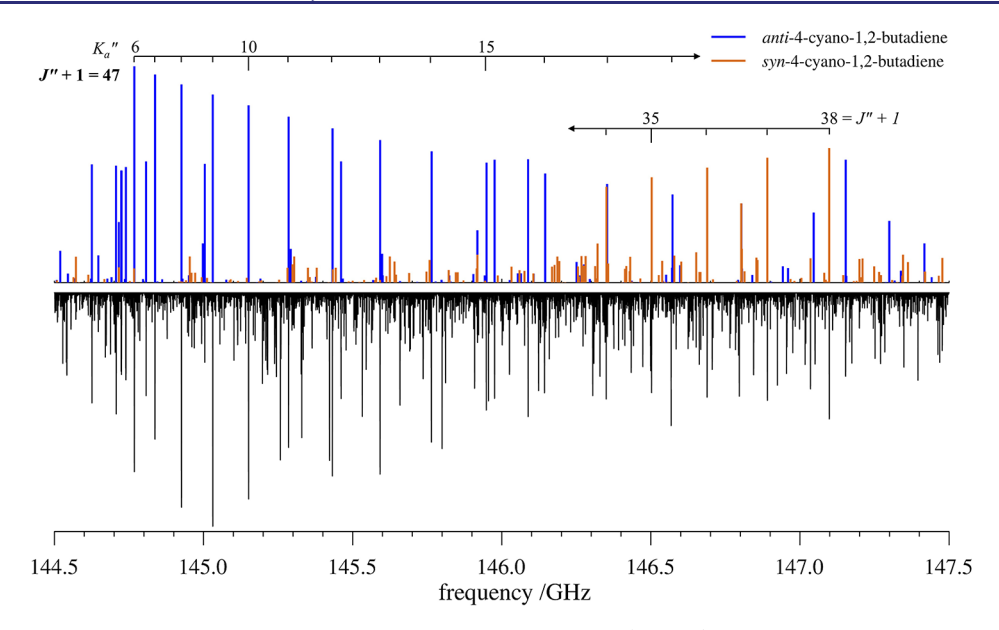


Figure 13. Rotational spectrum of 4-cyano-1,2-butadiene from 144.50 to 147.50 GHz (bottom) and stick spectrum of the ground vibrational state transitions (top). Blue lines mark transitions of *anti*-4-cyano-1,2-butadiene, and copper lines mark transitions of *syn*-4-cyano-1,2-butadiene. Many transitions belonging to other vibrational satellites are also visible in the experimental spectrum.

in the spectrum. The rotational transitions of the *syn* conformer exhibit a more regular spectral pattern (Figure 13). R-branch bandheads of the *syn* conformer begin quadruply degenerate (two ${}^aR_{0,1}$ transitions, ${}^bR_{1,1}$, ${}^bR_{-1,1}$) at $K_a = 0$ and 1 with all same values of K_c . Transitions proceed to lower frequency with increasing K_a , undergo a turnaround, and lose degeneracy. At higher values of K_a , the two a-type transitions with the same value of K_a become degenerate and the two b-type transitions with the same value of K_a become degenerate. Numerous Q-branch transitions are also observed in the spectrum of the syn conformer.

The ground vibrational state of the anti conformer of 4cyano-1,2-butadiene exhibits coupling in our spectral range. Most noticeably, ${}^{a}R_{0,1}$ transitions of the $K_{a} = 18$ series exhibit deviation from their distorted-rotor-predicted frequencies in a manner that does not follow a consistent pattern across values of J. During initial fitting, transitions of this series appeared well-predicted at J'' + 1 = 50, deviated to increasingly lower frequencies with increasing I, and reached a maximum deviation at J'' + 1 = 93. At even higher values of J, the transitions reapproached their predicted frequencies and appeared reasonably predicted near J'' + 1 = 115. Such a pattern of deviations cannot be addressed by including more distortion constants in the least-squares fit. As was done for strans-E-1-cyano-1,3-butadiene, transitions that were evidently perturbed or had quantum-number values proximate to those of clearly perturbed transitions (all $K_a > 12$) were excluded from the data set presented here to acquire minimally perturbed spectroscopic constants. The resultant data set includes R-branch transitions ranging in J" from 5 to 123 and K_a " from 0 to 12, as well as Q-branch transitions that range in J'' from 21 to 67 and K_a'' from 6 to 8. The corresponding data distribution plot is provided in Figure 14a. The ground vibrational state of the syn conformer, on the other hand, appears to behave as a distorted rotor in the same frequency range. R-branch transitions assigned for this conformer range in J'' from 11 to 94 and K_a'' from 0 to 29 and Q-branch transitions range in J'' from 23 to 69 and K_a'' from 1 to 30. The

data distribution plot for the *syn-*4-cyano-1,2-butadiene ground vibrational state is provided in Figure 14b.

These data represent the first millimeter-wave observation and analysis of 4-cyano-1,2-butadiene. The ground vibrational states of both the anti and syn conformers are fit to partial octic, distorted-rotor Hamiltonians with low error ($\sigma_{\rm fit}$ < 0.05 MHz). Their spectroscopic constants are presented in Table 3. Although the least-squares fit for the anti conformer does not address the coupling observed in our frequency range, we expect that the constants are minimally affected by perturbation and physically meaningful (vide infra). A comparison of the predicted rotational and distortion constants with those from the minimally perturbed leastsquares fit is provided in Table 3, and the resultant fit files are provided in the Supporting Information. As with the other isomers, the spectroscopic constants predicted by the B3LYP anharmonic calculation are reasonably good estimates of the experimental constants. The A_0 rotational constant of the anti conformer is predicted within 2.2% of the value determined in the minimally perturbed least-squares fit; the values of B_0 and C_0 are within 1%. The quartic centrifugal distortion constants are predicted within 24% of the values obtained in the experimental fit, and the sextic centrifugal distortion constants are within 61% of the experimental values. Overall, these discrepancies between predicted and experimental constants are within the expected ranges, lending credence to the idea that most effects of perturbation have been minimized or avoided. This conclusion is reinforced by the fact that the predicted vs. experimental discrepancies for the anti conformer are smaller than those for the syn conformer, which was amenable to a single-state least-squares fit without indications of perturbation. The rotational constants of syn-4-cyano-1,2butadiene are within 2.8%-5.5% of their experimental values. The quartic centrifugal distortion constants are predicted within 27%, and the sextic constants are predicted within 61% of the experimentally determined values, with the exception of H_{IK} , which is predicted to be a little over 3 times larger than its fitted value. The large values of inertial defect for the anti and syn conformers (-23.9 and -6.3 uÅ², respectively; Table 3)

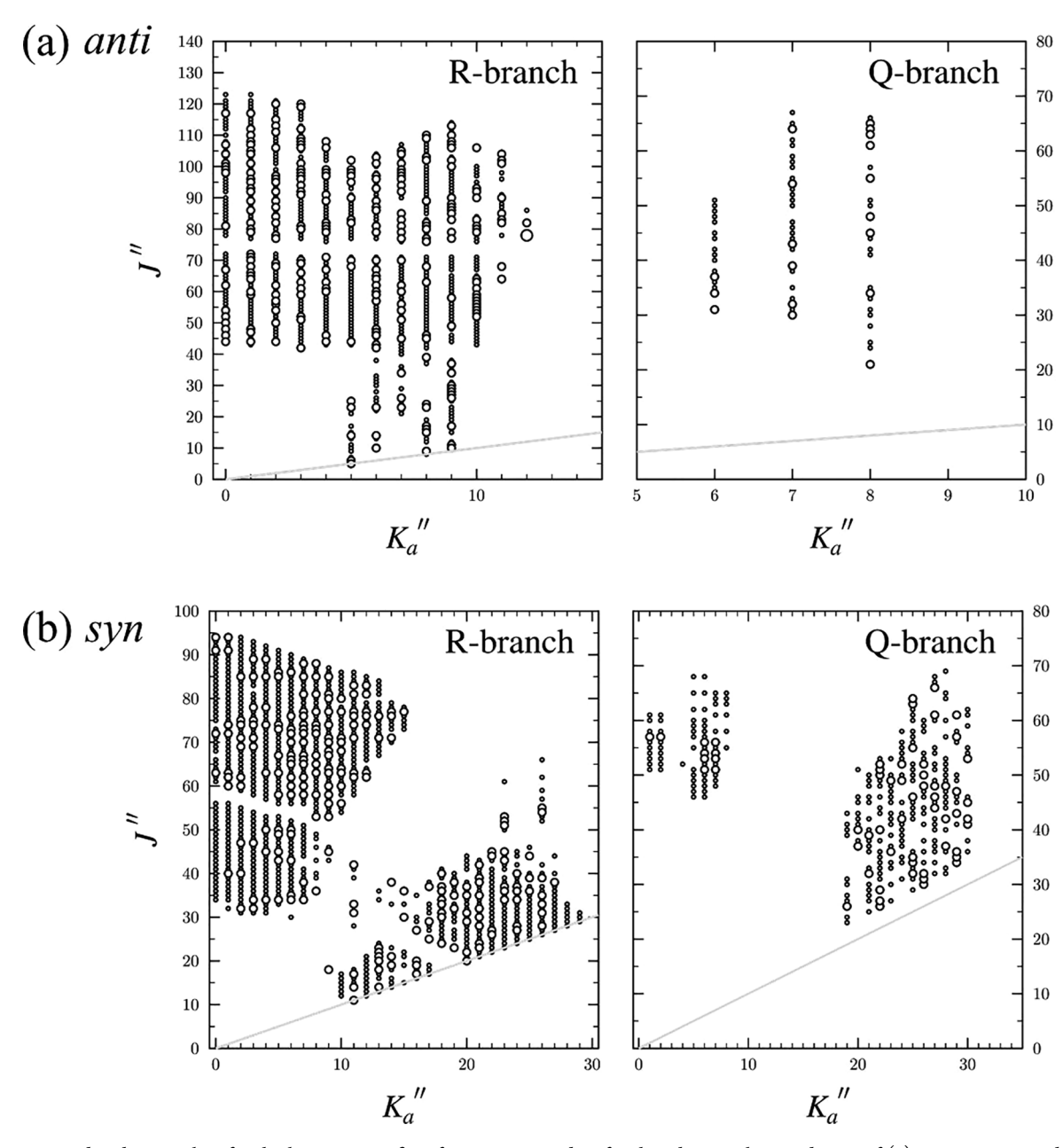


Figure 14. Data distribution plots for the least-squares fits of spectroscopic data for the vibrational ground state of (a) anti-4-cyano-1,2-butadiene and (b) syn-4-cyano-1,2-butadiene. Circles indicate Q- and R-branch transitions. The size of the plotted symbol is proportional to the value of $|(f_{obs} - f_{calc})/\delta f|$, where δf is the frequency measurement uncertainty (50 kHz); all values shown are smaller than 3.

are indicative of the nonplanarity of both species, as well as the significant structural differences between the two conformers.

Structural and Spectroscopic Comparisons. The cyanobutadiene isomers discussed in this work reveal interesting, and perhaps unanticipated, facets of the oftentimes complex relationships between structural and spectroscopic properties within a closely related family of molecules. In terms of molecular structure, the *E*- and *Z*-1-cyano-1,3-butadienes are quite similar: the connectivity of their atoms is the same, the conformational potential energy surfaces resemble one another in form and energetics, and the electronic distribution is similar, resulting in similar NMR and IR spectra. All of these features are distinct from those of 4-cyano-1,2-butadiene. In terms of molecular spectroscopy, however, the comparisons cut in a different direction. The rotational spectra of the *E*- and *Z*-1-cyano-1,3-butadienes are distinctly different because of

differing values of the asymmetry parameter ($\kappa = -0.99$ vs -0.91, respectively). The rotational spectra of the *anti*- and *syn*-4-cyano-1,2-butadienes are even more different, for the same reason ($\kappa = -0.99$ vs -0.60, respectively). The highly prolate character of *s*-trans-E-1-cyano-1,3-butadiene and *anti*-4-cyano-1,2-butadiene ($\kappa = -0.99$) sets these molecules apart from *s*-trans-Z-1-cyano-1,3-butadiene and *syn*-4-cyano-1,2-butadiene. Even within a closely related family of isomers, differences in molecular shape may lead to a disparate set of rotational spectra and spectroscopic constants (Table 4).

One significant difference among the rotational spectra in this study involves whether the rotational ground states are "isolated" (*i.e.*, not coupled to other states) in the observed frequency range or whether they exhibit coupling. Coupling becomes evident when rotational energies of one vibrational state are close to those of another vibrational state. For a

Table 3. Experimental and Computational Spectroscopic Constants for the Ground Vibrational States of anti- and syn-4-Cyano-1,2-butadiene (C_5H_5N) (S-Reduced Hamiltonian, I^r Representation)^e

	anti-4-cya	nno-1,2-butadiene	syn-4-cy	rano-1,2-butadiene
	B3LYP ^a	experimental	B3LYP ^a	experimental
A_0 (MHz)	14798	14498.4293 (34)	6187	5967.20395 (62)
B_0 (MHz)	1552	1567.06312 (17)	2575	2722.54115 (25)
C_0 (MHz)	1503	1515.78726 (13)	1860	1914.200040 (81)
D_I (kHz)	0.94	1.071171 (27)	2.7	3.278037 (57)
D _{JK} (kHz)	-64	-73.5948 (19)	-13.4	-14.49348 (57)
D_K (kHz)	1394	1611.957 (57)	23	22.1617 (23)
d_1 (kHz)	-0.195	-0.227538 (19)	-1.03	-1.305350 (30)
d_2 (kHz)	-0.0050	-0.006534 (10)	-0.062	-0.0849150 (95)
H_I (Hz)	0.0043	0.0070148 (28)	0.0123	0.0110340 (76)
H_{JK} (Hz)	-0.13	-0.31896 (19)	-0.048	-0.015533 (94)
H_{KI} (Hz)	-12	-11.206 (28)	-0.069	-0.17240 (99)
H_K (Hz)	362	397.33 (30)	0.27	0.3383 (33)
h_1 (Hz)	0.0019	0.0030023 (21)	0.00653	0.0062572 (45)
h_2 (Hz)	0.00019	0.0003851 (15)	0.00094	0.0011238 (21)
h_3 (Hz)	0.000012	0.00002934 (38)	0.00016	0.00020095 (51
L_{I} (μ Hz)		-0.05251 (10)		[0.0]
L_{IJK} (μ Hz)		3.4508 (96)		-0.237 (11)
L_{JK} (μ Hz)		-81.34 (99)		[0.0]
L_{KKJ} (μ Hz)	6390 (150)			4.94 (57)
$L_K (\mu Hz)$		[0.0]		-7.4 (1.7)
$l_1 (\mu Hz)$		-0.025404 (85)		[0.0]
$l_2 (\mu Hz)$		-0.004564 (63)		[0.0]
$l_3 (\mu Hz)$		-0.000833 (25)		[0.0]
$l_4 (\mu \text{Hz})$		[0.0]		[0.0]
$\Delta_i \left(\text{uÅ}^2 \right)^{b,c}$		-23.947986 (46)		-6.304674 (22)
$N_{ m lines}^{}$		1147		1172
$\sigma_{ m fit} \ ({ m MHz})$		0.043		0.038

^aEvaluated with the 6-311+G(2d,p) basis set. ^bInertial defect, $\Delta_i = I_c - I_a - I_b$. ^cCalculated by using PLANM from the B_0 constants. ^dNumber of fitted transition frequencies. ^eValues in square brackets held fixed in least-squares fit.

Table 4. Summary of Rotational Constants and Two Lowest-Energy Fundamentals for *s-trans-E-*1-Cyano-1,3-butadiene, *s-trans-Z-*1-Cyano-1,3-butadiene, *anti-*4-Cyano-1,2-butadiene (S-Reduced Hamiltonian, I^r Representation)

molecule	A_0 (MHz)	B_0 (MHz)	C_0 (MHz)	lowest-energy fundamentals ^a
s-trans-E-1-cyano-1,3-butadiene	26243.02934 (59)	1443.620880 (18)	1368.119206 (18)	$\nu_{19} \; ({\rm A'}, \; 138 \; {\rm cm}^{-1}, \; 141 \; {\rm cm}^{-1})$
				$\nu_{27} \; ({\rm A''}, \; 141 \; {\rm cm}^{-1}, \; 137 \; {\rm cm}^{-1})$
s-trans-Z-1-cyano-1,3-butadiene	9759.44594 (25)	2039.686938 (29)	1686.177389 (28)	$\nu_{19} \; ({\rm A'}, \; 127 \; {\rm cm}^{-1}, \; 129 \; {\rm cm}^{-1})$
				$\nu_{27} \; (\mathrm{A''}, \; 140 \; \mathrm{cm}^{-1}, \; 135 \; \mathrm{cm}^{-1})$
anti-4-cyano-1,2-butadiene	14498.4293 (34)	1567.06312 (17)	1515.78726 (13)	ν_{27} (A, 56 cm ⁻¹ , 53 cm ⁻¹)
				ν_{26} (A, 173 cm ⁻¹ , 170 cm ⁻¹)
syn-4-cyano-1,2-butadiene	5967.20395 (62)	2722.54115 (25)	1914.200040 (81)	$\nu_{27} \; (\text{A}'', 95 \; \text{cm}^{-1}, 86 \; \text{cm}^{-1})$
				$\nu_{17} \; ({\rm A'}, 105 \; {\rm cm}^{-1}, 103 \; {\rm cm}^{-1})$

^aB3LYP/6-311+G(2d,p). First value is energy from harmonic frequency calculation; second value is energy from anharmonic frequency calculation.

molecule with a given symmetry, the triple direct product of the irreducible representations of the interacting vibrations and the coupling interaction must equal the totally symmetric representation. In a C_s molecule, Fermi and c-type Coriolis coupling transform like the A' irreducible representation, while a- and b-type Coriolis coupling transform like the A' irreducible representation. For a molecule with no symmetry, all types of coupling are possible between any interacting states. The matter of whether or not coupling is observed is not just a detail of the spectroscopy; it is fundamental to the proper understanding of laboratory spectra and the use of these spectra as a basis for assigning species in astronomical or other harsh reaction environments. The

differing observations of coupling in our frequency range (absent for s-trans-Z-1-cyano-1,3-butadiene and syn-4-cyano-1,2-butadiene; present for s-trans-E-1-cyano-1,3-butadiene and anti-4-cyano-1,2-butadiene) result from several interacting factors. One factor that plays into the observation of coupling is the magnitude of the coupling constant(s). Even without predicting the coupling constants, however, the magnitudes of each molecule's A_0 and C_0 constants and the energy separations between states make it possible to rationalize the different spectroscopic behaviors (Table 4). A smaller energy separation between vibrational states increases the likelihood of proximity between their rotational levels. In the case of anti-4-cyano-1,2-butadiene, the lowest-energy vibrationally excited

state is predicted to be only 53 cm⁻¹ above the ground state less than half of the predicted energy separation in either E- or Z-1-cyano-1,3-butadiene. Although the energy separation between syn-4-cyano-1,2-butadiene and its lowest-energy fundamental is 86 cm⁻¹, which is also smaller than the predicted energy separation of either 1-cyano-1,3-butadiene ground state and fundamental, the lack of observed coupling can be rationalized by the magnitudes of the rotational constants. The larger the value of A_0 , the more widely spread the rotational energy levels for different K values of a vibrational state, and therefore the rotational energy levels of the lower-energy vibrational state approach those of the higher-energy state at lower K_a values. At the same time, the smaller the value of C_0 , the more closely spaced the rotational levels for different J values. As a result, higher values of J, which are more likely to exhibit coupling, are observed in a given frequency region. Indeed, of the isomers examined here, strans-E-1-cyano-1,3-butadiene exhibits the largest value of A_0 , the smallest value of C_0 , and observed R-branch transitions with the highest value of J (J'' = 134). anti-4-Cyano-1,2butadiene has the second-largest A_0 , second-smallest C_0 , and observed R-branch transitions with the second-highest value of I(I'' = 123). As a result, it is reasonable that these molecules exhibit coupling in our observed frequency region. Ground vibrational state coupling is not unfamiliar in rotational spectroscopy; other highly prolate molecules such as hydrazoic acid $(HN_3)^{57,58}$ and vinyl cyanide $(C_3H_3N)^{50,59}$ also show coupling between their ground and vibrationally excited states. These molecules similarly have large values of A_0 : 611 034.132 (29) MHz for hydrazoic acid⁶⁰ and 49 850.69655 (43) MHz for vinyl cyanide.50

CONCLUSIONS

In this work, we present a detailed analysis of the millimeterwave rotational spectra of E-1-cyano-1,3-butadiene, Z-1-cyano-1,3-butadiene, and 4-cyano-1,2-butadiene. Each of the observed conformers of these molecules has been fit to an octic, distorted-rotor Hamiltonian, and the resultant spectroscopic constants may be used for identification of these species in spectra of extraterrestrial sources and other harsh environments. Transitions for Z-1-cyano-1,3-butadiene and syn-4cyano-1,2-butadiene, which do not exhibit coupling in their ground states, are expected to be accurately predicted to 370 GHz for the entire range of quantum numbers observed in this work. Despite evidence of coupling in the ground states of strans-E-1-cyano-1,3-butadiene and anti-4-cyano-1,2-butadiene, the spectroscopic constants provided for these two molecules are expected to be minimally perturbed and sufficiently precise for detection of these molecules up to 370 GHz. For anti-4cyano-1,2-butadiene, it is expected that R-branch transitions with K_a up to 10 within this frequency range are well-predicted by the spectroscopic constants presented above. For s-trans-E-1-cyano-1,3-butadiene, this limit is slightly higher, such that Rbranch transitions with K_a values up to 15 are expected to be predicted within experimental accuracy by using the constants provided above. Indeed, the predicted spectra resulting from this work have already enabled identification of the s-trans conformers of E- and Z-1-cyano-1,3-butadiene as products in reaction spectra. 21,22

ASSOCIATED CONTENT

Supporting Information

The Supporting Information is available free of charge at https://pubs.acs.org/doi/10.1021/jacs.1c03777.

Directory of files; comparison of A reduction constants for *s-trans-Z-*1-cyano-1,3-butadiene, as determined in this work and in the work of McCarthy *et al.*²¹ (PDF) Least-squares fitting files of *E*-1-cyano-1,3-butadiene, *Z*-1-cyano-1,3-butadiene, and 4-cyano-1,2-butadiene; output files from computational studies (ZIP)

AUTHOR INFORMATION

Corresponding Authors

Robert J. McMahon — Department of Chemistry, University of Wisconsin—Madison, Madison, Wisconsin 53706, United States; orcid.org/0000-0003-1377-5107; Email: robert.mcmahon@wisc.edu

R. Claude Woods — Department of Chemistry, University of Wisconsin—Madison, Madison, Wisconsin 53706, United States; Email: rcwoods@wisc.edu

Authors

- Maria A. Zdanovskaia Department of Chemistry, University of Wisconsin–Madison, Madison, Wisconsin 53706, United States; orcid.org/0000-0001-5167-8573
- P. Matisha Dorman Department of Chemistry, University of Wisconsin–Madison, Madison, Wisconsin 53706, United States; orcid.org/0000-0003-3802-6719
- Vanessa L. Orr Department of Chemistry, University of Wisconsin–Madison, Madison, Wisconsin 53706, United States
- Andrew N. Owen Department of Chemistry, University of Wisconsin–Madison, Madison, Wisconsin 53706, United States
- Samuel M. Kougias Department of Chemistry, University of Wisconsin–Madison, Madison, Wisconsin 53706, United States; ⊚ orcid.org/0000-0002-9877-0817
- Brian J. Esselman Department of Chemistry, University of Wisconsin–Madison, Madison, Wisconsin 53706, United States; orcid.org/0000-0002-9385-8078

Complete contact information is available at: https://pubs.acs.org/10.1021/jacs.1c03777

Author Contributions

M.A.Z., P.M.D., and V.L.O. contributed equally to the spectroscopic analyses described in this work.

Notes

The authors declare no competing financial interest.

ACKNOWLEDGMENTS

We gratefully acknowledge funding from the National Science Foundation for support of this project (CHE-1664912 and CHE-1954270). P.M.D. thanks the University of Wisconsin—Madison Graduate School for support as an Advanced Opportunity Fellow. We thank Michael McCarthy for the loan of an Amplification-Multiplication Chain (WR5.1 AMC 530). We thank the Harvey Spangler Award (to B.J.E.) for the funding that supported the purchase of the Virginia Diodes Zero-Bias Detector (WR5.1ZBD 140–220 GHz). We thank Michael McCarthy, Kelvin Lee, Timothy Zwier, and Piyush Mishra for stimulating discussions.

■ REFERENCES

- (1) McGuire, B. A.; Burkhardt, A. M.; Kalenskii, S. V.; Shingledecker, C. N.; Remijan, A. J.; Herbst, E.; McCarthy, M. C. Detection of the Aromatic Molecule Benzonitrile (c-C₆H₅CN) in the Interstellar Medium. *Science* **2018**, 359, 202–205.
- (2) McCarthy, M. C.; Lee, K. L. K.; Loomis, R. A.; Burkhardt, A. M.; Shingledecker, C. N.; Charnley, S. B.; Cordiner, M. A.; Herbst, E.; Kalenskii, S.; Willis, E. R.; Xue, C.; Remijan, A. J.; McGuire, B. A. Interstellar detection of the highly polar five-membered ring cyanocyclopentadiene. *Nat. Astron.* **2021**, *5*, 176–180.
- (3) McGuire, B. A.; Loomis, R. A.; Burkhardt, A. M.; Lee, K. L. K.; Shingledecker, C. N.; Charnley, S. B.; Cooke, I. R.; Cordiner, M. A.; Herbst, E.; Kalenskii, S.; Siebert, M. A.; Willis, E. R.; Xue, C.; Remijan, A. J.; McCarthy, M. C. Detection of two interstellar polycyclic aromatic hydrocarbons via spectral matched filtering. *Science* 2021, 371, 1265–1269.
- (4) McCarthy, M. C.; McGuire, B. A. Aromatics and Cyclic Molecules in Molecular Clouds: A New Dimension of Interstellar Organic Chemistry. *J. Phys. Chem. A* **2021**, *125*, 3231–3243.
- (S) Halter, R. J.; Fimmen, R. L.; McMahon, R. J.; Peebles, S. A.; Kuczkowski, R. L.; Stanton, J. F. Microwave Spectra and Molecular Structures of (Z)-Pent-2-en-4-ynenitrile and Maleonitrile. *J. Am. Chem. Soc.* **2001**, *123*, 12353–12363.
- (6) Müller, H. S. P.; Schlöder, F.; Stutzki, J.; Winnewisser, G. The Cologne Database for Molecular Spectroscopy, CDMS: a Useful Tool for Astronomers and Spectroscopists. *J. Mol. Struct.* **2005**, 742, 215–227.
- (7) Endres, C. P.; Schlemmer, S.; Schilke, P.; Stutzki, J.; Müller, H. S. P. The Cologne Database for Molecular Spectroscopy, CDMS, in the Virtual Atomic and Molecular Data Centre. *J. Mol. Spectrosc.* **2016**, 327, 95–104.
- (8) Avery, L. W.; Broten, N. W.; MacLeod, J. M.; Oka, T.; Kroto, H. W. Detection of the Heavy Interstellar Molecule Cyanodiacetylene. *Astrophys. J.* **1976**, 205, L173–L175.
- (9) Broten, N. W.; Oka, T.; Avery, L. W.; MacLeod, J. M.; Kroto, H. W. The Detection of Cyanooctatetrayne (HC₉N) in Interstellar Space. *Astrophys. J.* **1978**, 223, L105–L107.
- (10) Kroto, H. W.; Kirby, C.; Walton, D. R. M.; Avery, L. W.; Broten, N. W.; MacLeod, J. M.; Oka, T. The Detection of Cyanohexatriyne, $H(C \equiv C)_3 CN$, in Heiles's Cloud 2. *Astrophys. J.* 1978, 219, L133–L137.
- (11) Snyder, L. E.; Buhl, D. Radio Emission from Interstellar Hydrogen Cyanide. *Astrophys. J.* **1971**, *163*, L47–L52.
- (12) Walmsley, C. M.; Winnewisser, G.; Toelle, F. Cyanoacetylene and Cyanodiacetylene in Interstellar Clouds. *Astron. Astrophys.* **1980**, *81*, 245–50.
- (13) Loomis, R. A.; Burkhardt, A. M.; Shingledecker, C. N.; Charnley, S. B.; Cordiner, M. A.; Herbst, E.; Kalenskii, S.; Lee, K. L. K.; Willis, E. R.; Xue, C.; Remijan, A. J.; McCarthy, M. C.; McGuire, B. A. An investigation of spectral line stacking techniques and application to the detection of $HC_{11}N$. *Nat. Astron.* **2021**, *5*, 188–196.
- (14) Broten, N. W.; MacLeod, J. M.; Avery, L. W.; Irvine, W. M.; Hoeglund, B.; Friberg, P.; Hjalmarson, A. The Detection of Interstellar Methylcyanoacetylene. *Astrophys. J.* **1984**, *276*, L25–L29. (15) Gardner, F. F.; Winnewisser, G. Detection of Interstellar Vinyl
- Cyanide (Acrylonitrile). *Astrophys. J.* **1975**, 195, L127–L130.
- (16) Snyder, L. E.; Hollis, J. M.; Jewell, P. R.; Lovas, F. J.; Remijan, A. Confirmation of Interstellar Methylcyanodiacetylene (CH₃C₅N). *Astrophys. J.* **2006**, 647, 412–417.
- (17) Lovas, F. J.; Remijan, A. J.; Hollis, J. M.; Jewell, P. R.; Snyder, L. E. Hyperfine Structure Identification of Interstellar Cyanoallene Toward TMC-1. *Astrophys. J.* **2006**, *637*, L37–L40.
- (18) Solomon, P. M.; Jefferts, K. B.; Penzias, A. A.; Wilson, R. W. Detection of Millimeter Emission Lines from Interstellar Methyl Cyanide. *Astrophys. J.* **1971**, *168*, L107–L110.
- (19) Belloche, A.; Garrod, R. T.; Müller, H. S. P.; Menten, K. M. Detection of a Branched Alkyl Molecule in the Interstellar Medium: iso-Propyl Cyanide. Science 2014, 345, 1584–1587.

- (20) Belloche, A.; Garrod, R. T.; Müller, H. S. P.; Menten, K. M.; Comito, C.; Schilke, P. Increased Complexity in Interstellar Chemistry: Detection and Chemical Modeling of Ethyl Formate and *n*-Propyl Cyanide in Sagittarius B2(N). *Astron. Astrophys.* **2009**, 499, 215–232.
- (21) McCarthy, M. C.; Lee, K. L. K.; Carroll, P. B.; Porterfield, J. P.; Changala, P. B.; Thorpe, J. H.; Stanton, J. F. Exhaustive Product Analysis of Three Benzene Discharges by Microwave Spectroscopy. *J. Phys. Chem. A* **2020**, *124*, 5170–5181.
- (22) Mishra, P.; Fritz, S. M.; Herbers, S.; Mebel, A. M.; Zwier, T. S. Gas-Phase Pyrolysis of *trans* 3-Pentenenitrile: Competition between Direct and Isomerization-Mediated Dissociation. *Phys. Chem. Chem. Phys.* **2021**, 23, 6462–6471.
- (23) Tsukamoto, A.; Lichtin, N. N., Reactions of Active Nitrogen with Organic Substrates. I. The Monomeric Products of the Reaction with 1,3-Butadiene. *J. Am. Chem. Soc.* **1962**, *84*, 1601–1605.
- (24) Sun, B. J.; Huang, C. H.; Chen, S. Y.; Chen, S. H.; Kaiser, R. I.; Chang, A. H. H. Theoretical Study on Reaction Mechanism of Ground-State Cyano Radical with 1,3-Butadiene: Prospect of Pyridine Formation. *J. Phys. Chem. A* **2014**, *118*, 7715–7724.
- (25) Morales, S. B.; Bennett, C. J.; Le Picard, S. D.; Canosa, A.; Sims, I. R.; Sun, B. J.; Chen, P. H.; Chang, A. H. H.; Kislov, V. V.; Mebel, A. M.; Gu, X.; Zhang, F.; Maksyutenko, P.; Kaiser, R. I. A Crossed Molecular Beam, Low-Temperature Kinetics, And Theoretical Investigation Of The Reaction Of The Cyano Radical (CN) With 1,3-Butadiene (C_4H_6). A Route To Complex Nitrogen-Bearing Molecules In Low-Temperature Extraterrestrial Environments. Astrophys. J. 2011, 742, 26.
- (26) McKellar, A. Evidence for the Molecular Origin of Some Hitherto Unidentified Interstellar Lines. *Publ. Astron. Soc. Pac.* **1940**, 52, 187.
- (27) Baraban, J. H.; Martin-Drumel, M.-A.; Changala, P. B.; Eibenberger, S.; Nava, M.; Patterson, D.; Stanton, J. F.; Ellison, G. B.; McCarthy, M. C. The Molecular Structure of *gauche-1,3*-Butadiene: Experimental Establishment of Non-planarity. *Angew. Chem., Int. Ed.* **2018**, *57*, 1821–1825.
- (28) Balucani, N.; Asvany, O.; Huang, L. C. L.; Lee, Y. T.; Kaiser, R. I.; Osamura, Y.; Bettinger, H. F. Formation of Nitriles in the Interstellar Medium via Reactions of Cyano Radicals, $CN(X^{2}\Sigma^{+})$, with Unsaturated Hydrocarbons. *Astrophys. J.* **2000**, *545*, 892–906.
- (29) Jamal, A.; Mebel, A. M. Theoretical Investigation of the Mechanism and Product Branching Ratios of the Reactions of Cyano Radical with 1- and 2-Butyne and 1,2-Butadiene. *J. Phys. Chem. A* **2013**, *117*, 741–755.
- (30) Esselman, B. J.; Zdanovskaia, M. A.; Kougias, S. M.; Patel, A. R.; Woods, R. C.; McMahon, R. J. The 130–360 GHz Rotational Spectrum of syn-2-Cyano-1,3-Butadiene (C_5H_5N) A Molecule of Astrochemical Relevance, manuscript submitted.
- (31) Sagan, C.; Thompson, W. R.; Khare, B. N. Titan: a laboratory for prebiological organic chemistry. *Acc. Chem. Res.* **1992**, *25*, 286–292
- (32) Waite, J. H.; Niemann, H.; Yelle, R. V.; Kasprzak, W. T.; Cravens, T. E.; Luhmann, J. G.; McNutt, R. L.; Ip, W.-H.; Gell, D.; De La Haye, V.; Müller-Wordag, I.; Magee, B.; Borggren, N.; Ledvina, S.; Fletcher, G.; Walter, E.; Miller, R.; Scherer, S.; Thorpe, R.; Xu, J.; Block, B.; Arnett, K. Ion Neutral Mass Spectrometer Results from the First Flyby of Titan. *Science* 2005, 308, 982–986.
- (33) Waite, J. H.; Young, D. T.; Cravens, T. E.; Coates, A. J.; Crary, F. J.; Magee, B.; Westlake, J. The Process of Tholin Formation in Titan's Upper Atmosphere. *Science* **2007**, *316*, 870–875.
- (34) Desai, R. T.; Coates, A. J.; Wellbrock, A.; Vuitton, V.; Crary, F. J.; González-Caniulef, D.; Shebanits, O.; Jones, G. H.; Lewis, G. R.; Waite, J. H.; Cordiner, M.; Taylor, S. A.; Kataria, D. O.; Wahlund, J.-E.; Edberg, N. J. T.; Sittler, E. C. Carbon chain anions and the growth of complex organic molecules in Titan's ionosphere. *Astrophys. J., Lett.* **2017**, *844*, L18.
- (35) McGuigan, M.; Waite, J. H.; Imanaka, H.; Sacks, R. D. Analysis of Titan tholin pyrolysis products by comprehensive two-dimensional

- gas chromatography-time-of-flight mass spectrometry. J. Chromatogr. A 2006, 1132, 280-288.
- (36) Morisson, M.; Szopa, C.; Carrasco, N.; Buch, A.; Gautier, T. Titan's organic aerosols: Molecular composition and structure of laboratory analogues inferred from pyrolysis gas chromatography mass spectrometry analysis. Icarus 2016, 277, 442-454.
- (37) Nixon, C. A.; Thelen, A. E.; Cordiner, M. A.; Kisiel, Z.; Charnley, S. B.; Molter, E. M.; Serigano, J.; Irwin, P. G.; Teanby, N. A.; Kuan, Y.-J. Detection of Cyclopropenylidene on Titan with ALMA. Astron. J. 2020, 160, 205.
- (38) Charnley, S. B.; Kuan, Y.-J.; Huang, H.-C.; Botta, O.; Butner, H. M.; Cox, N.; Despois, D.; Ehrenfreund, P.; Kisiel, Z.; Lee, Y.-Y.; Markwick, A. J.; Peeters, Z.; Rodgers, S. D. Astronomical Searches for Nitrogen Heterocycles. Adv. Space Res. 2005, 36, 137-145.
- (39) Cyanopyridine isomers represent alternate proxies for pyridine.
- (40) Dorman, P. M.; Esselman, B. J.; Park, J. E.; Woods, R. C.; McMahon, R. J. Millimeter-wave spectrum of 4-cyanopyridine in its ground state and lowest-energy vibrationally excited states, ν_{20} and ν_{30} . I. Mol. Spectrosc. **2020**, 369, 111274.
- (41) Dorman, P. M.; Esselman, B. J.; Woods, R. C.; McMahon, R. J. An analysis of the rotational ground state and lowest-energy vibrationally excited dyad of 3-cyanopyridine: Low symmetry reveals rich complexity of perturbations, couplings, and interstate transitions. J. Mol. Spectrosc. 2020, 373, 111373.
- (42) Raffaelli, N. Nicotinamide Coenzyme Synthesis: A Case of Ribonucleotide Emergence or a Byproduct of the RNA World?. In Origins of Life: The Primal Self-Organization; Egel, R., Lankenau, D.-H., Mulkidjanian, A. Y., Eds.; Springer-Verlag: Heidelberg, 2011; p
- (43) McMurtry, B. M.; Turner, A. M.; Saito, S. E. J.; Kaiser, R. I. On the formation of niacin (vitamin B3) and pyridine carboxylic acids in interstellar model ices. Chem. Phys. 2016, 472, 173-184.
- (44) Pizzarello, S.; Huang, Y. The deuterium enrichment of individual amino acids in carbonaceous meteorites: A case for the presolar distribution of biomolecule precursors. Geochim. Cosmochim. Acta 2005, 69, 599-605.
- (45) Pizzarello, S.; Huang, Y.; Fuller, M. The carbon isotopic distribution of Murchison amino acids. Geochim. Cosmochim. Acta 2004, 68, 4963-4969.
- (46) Parker, D. S. N.; Kaiser, R. I. On the formation of nitrogensubstituted polycyclic aromatic hydrocarbons (NPAHs) in circumstellar and interstellar environments. Chem. Soc. Rev. 2017, 46, 452-
- (47) Kougias, S. M.; Knezz, S. N.; Owen, A. N.; Sanchez, R. A.; Hyland, G. E.; Lee, D. J.; Patel, A. R.; Esselman, B. J.; Woods, R. C.; McMahon, R. J. Synthesis and Characterization of Cyanobutadiene Isomers-Molecules of Astrochemical Significance. J. Org. Chem. **2020**, *85*, 5787-5798.
- (48) Esselman, B. J.; Amberger, B. K.; Shutter, J. D.; Daane, M. A.; Stanton, J. F.; Woods, R. C.; McMahon, R. J. Rotational Spectroscopy of Pyridazine and its Isotopologs from 235-360 GHz: Equilibrium Structure and Vibrational Satellites. J. Chem. Phys. 2013, 139, 224304.
- (49) Zdanovskaia, M. A.; Esselman, B. J.; Woods, R. C.; McMahon, R. J. The 130 - 370 GHz Rotational Spectrum of Phenyl Isocyanide (C₆H₅NC). J. Chem. Phys. **2019**, 151, No. 024301.
- (50) Kisiel, Z.; Pszczółkowski, L.; Drouin, B. J.; Brauer, C. S.; Yu, S.; Pearson, J. C.; Medvedev, I. R.; Fortman, S.; Neese, C. Broadband rotational spectroscopy of acrylonitrile: Vibrational energies from perturbations. J. Mol. Spectrosc. 2012, 280, 134-144.
- (51) Kisiel, Z.; Pszczółkowski, L.; Medvedev, I. R.; Winnewisser, M.; De Lucia, F. C.; Herbst, E. Rotational spectrum of trans-trans diethyl ether in the ground and three excited vibrational states. J. Mol. Spectrosc. 2005, 233, 231-243.
- (52) Pickett, H. M. The fitting and prediction of vibration-rotation spectra with spin interactions. J. Mol. Spectrosc. 1991, 148, 371-377.
- (53) Kisiel, Z. PROSPE Programs for ROtational SPEctroscopy; http://info.ifpan.edu.pl/~kisiel/prospe.htm (accessed 2020-01-22).
- (54) Frisch, M. J.; Trucks, G. W.; Schlegel, H. B.; Scuseria, G. E.; Robb, M. A.; Cheeseman, J. R.; Scalmani, G.; Barone, V.; Petersson,

- G. A.; Nakatsuji, H.; Li, X.; Caricato, M.; Marenich, A. V.; Bloino, J.; Janesko, B. G.; Gomperts, R.; Mennucci, B.; Hratchian, H. P.; Ortiz, J. V.; Izmaylov, A. F.; Sonnenberg, J. L.; Williams-Young, D.; Ding, F.; Lipparini, F.; Egidi, F.; Goings, J.; Peng, B.; Petrone, A.; Henderson, T.; Ranasinghe, D.; Zakrzewski, V. G.; Gao, I.; Rega, N.; Zheng, G.; Liang, W.; Hada, M.; Ehara, M.; Toyota, K.; Fukuda, R.; Hasegawa, J.; Ishida, M.; Nakajima, T.; Honda, Y.; Kitao, O.; Nakai, H.; Vreven, T.; Throssell, K.; Montgomery, J. A., Jr.; Peralta, J. E.; Ogliaro, F.; Bearpark, M. J.; Heyd, J. J.; Brothers, E. N.; Kudin, K. N.; Staroverov, V. N.; Keith, T. A.; Kobayashi, R.; Normand, J.; Raghavachari, K.; Rendell, A. P.; Burant, J. C.; Ivengar, S. S.; Tomasi, J.; Cossi, M.; Millam, J. M.; Klene, M.; Adamo, C.; Cammi, R.; Ochterski, J. W.; Martin, R. L.; Morokuma, K.; Farkas, O.; Foresman, J. B.; Fox, D. J. Gaussian 16, Revision C.01; Gaussian, Inc.: Wallingford, CT, 2019. (55) Wilson, E. B., Jr.; Decius, J. C.; Cross, P. C. Molecular
- Vibrations; Dover: New York, 1980.
- (56) Gordy, W.; Cook, R. L. Microwave Molecular Spectra, 3rd ed.; Wiley-Interscience: New York, 1984.
- (57) Amberger, B. K. Millimeter-wave Spectroscopy of Highly Nitrogenous Molecules of Potential Astrochemical Interest. Ph.D. Thesis, University of Wisconsin-Madison, Madison, WI, 2015.
- (58) Vávra, K.; Kania, P.; Koucký, J.; Kisiel, Z.; Urban, Š. Rotational spectra of hydrazoic acid. J. Mol. Spectrosc. 2017, 337, 27-31.
- (59) Kisiel, Z.; Martin-Drumel, M.-A.; Pirali, O. Lowest vibrational states of acrylonitrile from microwave and synchrotron radiation spectra. I. Mol. Spectrosc. 2015, 315, 83-91.
- (60) Amberger, B. K.; Esselman, B. J.; Stanton, J. F.; Woods, R. C.; McMahon, R. J. Precise Equilibrium Structure Determination of Hydrazoic Acid (HN₃) by Millimeter-wave Spectroscopy. J. Chem. Phys. 2015, 143, 104310.